A Soft-switched Hybrid DC Circuit Breaker for the Protection of Fusion Power Plant Electrical Systems

Zhang, Hanwen; Ferro, Alberto; Franke, Thomas; Dan, Mattia; Terlizzi, Cristina; Wang, Yanbo; Chen, Zhe

Published in:
CIGRE Paris Session 2024

Publication date:
2024

Document Version
Accepted author manuscript, peer reviewed version

EUROFUSION WPPES-CPR(24) 36764

HZ Zhang et al.

A Soft-switched Hybrid DC Circuit Breaker for Fast Discharge Units in Fusion Power Plants

Preprint of Paper to be submitted for publication in Special Issue of CIGRE 2024 Paris Session

This work has been carried out within the framework of the EUROfusion Consortium and has received funding from the Euratom research and training programme 2014-2018 and 2019-2020 under grant agreement No 633053. The views and opinions expressed herein do not necessarily reflect those of the European Commission.

2024 Paris Session

Here your Paper ID – 5 numbers
B4 DC systems and power electronics
PS2 FACTS and power electronics

A Soft-switched Hybrid DC Circuit Breaker for Fast Discharge Units in Fusion Power Plants

Hanwen ZHANG*
Aalborg University
Denmark
hzha@energy.aau.dk

Ferro ALBERTO
Consorzio RFX
Italy
alberto.ferro@igi.cnr.it

Thomas FRANKE
Max-Planck-Institute for Plasma Physics
Germany
Thomas.Franke@euro-fusion.org

Mattia DAN
Consorzio RFX
Italy
mattia.dan@igi.cnr.it

Cristina TERLIZZI
University of Rome Tor Vergata
Italy
cristina.terlizzi@uniroma2.it

Yanbo WANG
Aalborg University
Denmark
ywa@energy.aau.dk

Zhe CHEN
Aalborg University
Denmark
zch@energy.aau.dk

SUMMARY

In recent years, the Danish nuclear fusion energy research programme has been supporting the ITER project in France, and contributing to EUROfusion activities, for a DEMOnstration fusion power plant. DEMO aims to showcase advanced technologies for controlling powerful fusion plasma and safely generating electricity within the range of 300 to 500 megawatts to the external grid and to supply its own electrical power systems. The fast discharge unit (FDU) is the core device in the quench protection system for protecting superconducting magnets. It is used to interrupt the DC current to avoid irreversible damage to the superconducting coils caused by overheating. In the planning phase, the designed operation current of central solenoid (CS) and poloidal field (PF) coils in DEMO is 45 kA, and the current of toroidal field (TF) coils is 74.6 kA.

This paper presents a soft-switched hybrid DC circuit breaker (CB) for FDUs in DEMO. The proposed CB comprises a mechanical bypass switch, an integrated gate-commutated thyristor (IGCT)-based static CB, and a thyristor-based counter pulse circuit. During the DC interrupting process, this design ensures a reliable zero current switching (ZCS) turn-off of the parallel connected IGCTs and thyristors, which avoids the risk of gate voltage oscillations and asymmetrical operations. The proposed DCCB offers two current interruption schemes for the FDU according to quench conditions, to improve reliability. A temperature-dependent discharge resistor made of mild steel is considered in this design. Compared to the constant-resistance solution, it can reduce the resistance of the discharge resistor. Therefore, the voltage peak applied to the coil is significantly reduced. The theoretical analysis and feasibility study of the proposed hybrid DCCB regarding each main component are presented. Simulation tests are conducted in PLECS under various conditions to verify the effectiveness of the proposed DCCB.

KEYWORDS

DC circuit breaker, fusion devices, quench protection circuits, DC fault protection.

ACKNOWLEDGEMENT

This work has been carried out within the framework of the EUROfusion Consortium, funded by the European Union via the Euratom Research and Training Programme (Grant Agreement No 101052200 — EUROfusion). Views and opinions expressed are however those of the author(s) only and do not necessarily reflect those of the European Union or the European Commission. Neither the European Union nor the European Commission can be held responsible for them.

I. Introduction

Accelerating the transition to a low-carbon society is a global priority. In this transition, fusion power is in line with the roadmap for environmental sustainability to generate power in a flexible, clean, and inexhaustible manner [1]. The concept of the tokamak originated in the 1950s. In the magnetic confinement fusion, a plasma is confined by controllable magnetic fields, provided, in the newest machines, by superconducting (SC) magnets [2].

Among those, ITER will be the largest experimental tokamak nuclear fusion reactor in the world. The ITER magnet combined magnetic energy of 51 GJ, which consists of 18 toroidal field (TF) coils, one central solenoid (CS) and six poloidal field (PF) coils [3]. In JT-60SA tokamak, the SC coil's rated current is 26 kA, and the heating and current drive power up to 41 MW [4]. The parameters of the SC magnet in CRAFT are 10 kV/100 kA with the range of fusion power from 50 MW to 200 MW [5]. The DEMOnstration fusion power plant (DEMO) will go from a science-driven experiment to a public-private partnership project with the involvement of industry from the beginning. [6], [7]. It is planned to generate electricity within the range of 300 to 500 MW to power systems and to supply its plant electrical power systems [8].

In all existing SC machines designed for long pulse experiments, SC coils must operate below the conditions of the superconductor material. If the condition is no longer met in the region, the transition from superconductivity to the normal resistive state will occur (so-called "quench") [9]. This can result in a high local temperature in the coil, potentially resulting in melting and the destruction of the coil. In the DEMO plant electrical system, the Fast Discharge Unit (FDU) is the key component to protect the SC coils as integrated into the coil power supply (CPS) system from the onset of the DEMO's design [10]. The primary function of FDU is to safeguard the SC coils by rapidly discharging the magnetic energy in the case of quench or fault to avoid the risk of potential damage to the SC coils.

The interruption of high DC current under high voltage is a challenging task in fusion devices. The main requirements for the DC circuit breaker (CB) in FDU are to conduct the current during the steady state operation with ultra-low power losses and to interrupt the current at the designed peak voltage level. In DEMO, the tentative rated current for all CS/PF coils is 45 kA. Specifically, for CS1U, CS1L, CS2U, CS2L, CS3U, CS3U, PF1, and PF6, the rated voltage is ±8 kV; and ±10 kV for PF2, PF3, PF4, and PF5. The baseline rating for TF coils is tentatively set at 74.6 kA. The discharge time constants of CS and PF coils are 7.5s and 15s respectively. The discharge time constant of TF coils is 35s [11]. Therefore, the design of FDU should not only satisfy the operational parameters but also meet the high requirements of reliability, availability, maintainability and inspectability (RAMI). TABLE I shows the parameters and the adopted DC current interruption technologies in long-pulse fusion devices.

TABLE I. Parameters of DC Protection Switches in Fusion Devices

Devices	Voltage (kV)	Current (kA)	CB technology
EAST [12]	3	15	mechanical switches + fuse-based CB
W7-X [13]	8	20	mechanical switches
JT60-SA [14]	5	25.7	BPS + full-controlled IGCTs
KSTAR [15]	8	40	mechanical switches+ auxiliary circuit
ITER [16]	10/24 (tested)	70/80 (tested)	BPS + VCB + auxiliary circuit
CRAFT [17]	10	100	ITER-like
CFETR [18]	20	100	mechanical + full-controlled IGBTs

In TABLE I, the DCCB in FDUs can be classified into three different categories: mechanical circuit breaker (MCB) e.g. EAST and W7-X; solid state circuit breaker (SSCB) e.g. the IGCT branch in JT60-SA; and hybrid circuit breaker (HCB) e.g. ITER, CRAFT, and CFETR. The classification is based on different current commutation methods and current breaking technologies. Furthermore, DCCBs can be subdivided into direct interruption CB and artificial zero-crossing commutation CBs. Typically, artificial zero-crossing commutation CBs contain a counter pulse circuit (CPC) network to create an artificial zero crossing to help extinguish the arc in the CB.

Among the different CBs, the ITER-like FDU is a proven technology which is suitable for high current and high voltage SC coils. The FDU comprises a mechanical bypass switch (BPS) in parallel to vacuum circuit breakers (VCBs). In the case of quench, the coil protection system initiates the FDU breaking process. The first step is to open the BPS. Hereafter, the BPS forces the current to be commutated to the closed contacts of the VCB. The VCB is actuated to open when the distance of the BPS contacts is sufficient to sustain the voltage. Then, the thyristors in the CPC are triggered to generate a pulse current in VCBs in the opposite direction to the coil current. As a result, when the current in the VCB decreases to zero, the current is naturally commutated into the discharge resistor (DR) [16]

In order to interrupt the current rapidly and safely, an SSCB is utilised in JT60-SA. The CB comprises a BPS and an SSCB branch in parallel. The SSCB consists of integrated gate-commutated thyristor (IGCT) stacks in antiparallel which are equipped with snubber network and passive components. This scheme has only two current commutation paths and adopts full-controlled power semiconductor devices. The SSCB structure features promising flexibility and maintainable properties [19]. However, in higher power rating applications such as DEMO, the utilisation of a large number of IGCT stacks is inevitable. In this case, the reliable turn-on/off is a challenging task even with high voltage applied [20]. For the IGCTs, equal current sharing must be ensured under on-state and transient conditions [21]. Although a symmetrical structure layout can ensure the consistency of the stray parameters, the synchronisation of gate signals and avoiding gate voltage oscillations are of importance for this scheme [22]. In W7-X and EAST, mechanical switches and fuses are used in FDUs. One important advantage of MCBs is they feature higher reliability and the ability to withstand high levels of neutron radiation. However, the MCBs are more capable of lower power rating SC coil applications.

The design of the FDU is related not only to the current rating but also to the reapplied voltage on the DR during the current interrupting process. A higher resistance at normal temperature e.g., 20℃, will result in higher peak voltage applied on the CB at the beginning of the FDU intervention. Thus, the capacity of the FDU is increased, resulting in complicated thermal optimisation and substantial dimensions. The DR unit is preferred to have a high-temperature coefficient and acceptable dimensions, which should be considered in the FDU design.

To meet the requirement of FDU in DEMO, a soft-switched hybrid DCCB is proposed in this paper. The proposed CB comprises a mechanical bypass switch, an IGCT-based static CB, and a CPC. In this design, IGCTs and thyristors are able to switch under ZCS conditions, which avoids gate voltage oscillations under high current conditions. This scheme reduces the transient power on switches with a fast operation, which enhances the reliability of IGCTs. A temperature-dependent discharge resistor made of mild steel is considered in this design to reduce the peak voltage applied to the FDU. In addition, the proposed CB can still directly and safely interrupt the DC current through the IGCT-based static CB under low current conditions. Therefore, the two current interruption schemes offer flexible options for the FDU according to quench conditions. The current commutation principle of the proposed FDU is presented. The parameter design and feasibility study are carried out in terms of DEMO's tentative design. The protection methods are verified and tested up to 45kA/20kV through simulations performed in PLECS/Plexim in different scenarios. The proposed FDU has high current interruption capability, low reapplied voltage, and improved flexibility.

II. The proposed FDU scheme and current commutation principle

A. The proposed FDU topology

Fig. 1 shows the proposed FDU in the CPS system. In DEMO, each SC coil is supplied by 4-quadrant thyristors-based converter. The initial ratings for DEMO CS/PF base converters are detailed in [11]. The proposed FDU comprises five parts: BPS, IGCT based CB, a thyristor-triggered CPC, and backup protection pyrobreaker. It is important to highlight that the topology should be designed in a symmetrical configuration to interrupt bidirectional current in CS/PF coils.

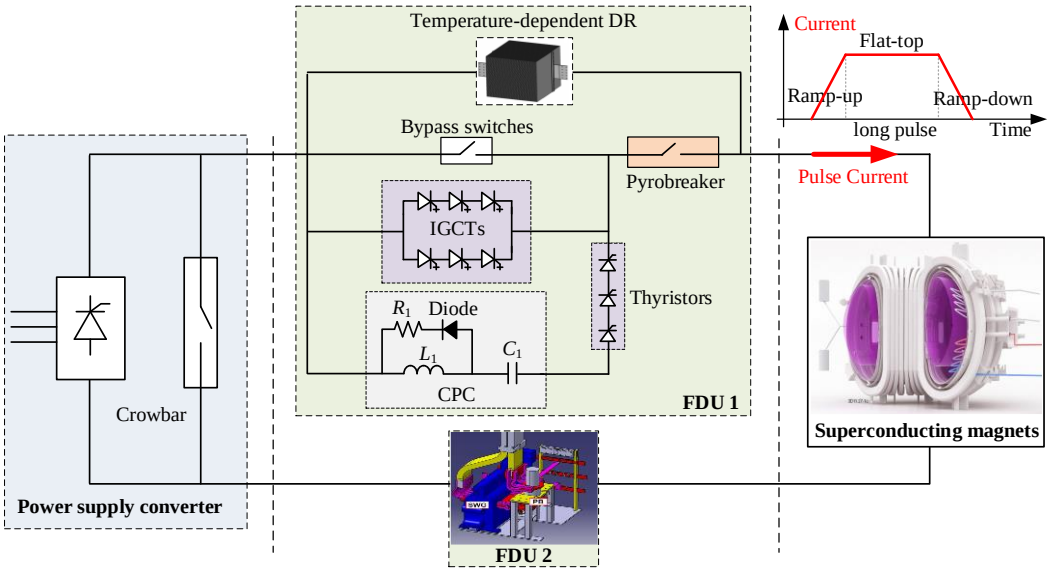

Fig.1 The proposed of FDU scheme with soft-switched hybrid CB.

In this design, the BPS is a mechanical switch with a pneumatic drive, carrying the steady-state coil current under normal operating conditions and featuring low power losses. The BPS in ITER has been tested up to 80 kA/ 24 kV [16]. It includes 12 low-resistance 6 kA main contacts.

The IGCT-based SSCB is composed of IGCTs connected in series and in parallel. The quantity of devices in series depends on the peak voltage applied to the CB. The number of IGCT branches in parallel is determined by considering worst-case current unbalance scenarios. Additionally, this design should take into account the inclusion of protection features such as antiparallel free-wheeling diodes, shunt resistors, and redundant branches. In the case of JT-60SA, a 25.7 kA IGCT-based CB has been successfully designed and tested. However, the proposed scheme necessitates connecting more IGCTs in parallel to meet the requirement.

The CPC is composed of a pre-charged capacitor bank (C_1), inductor (L_1) with discharge circuit (R_1, diodes), and high-power thyristors (TH). Similar to the ITER-like design, the CPC is parallel to the SSCB, and its actuation is controlled by triggering the thyristor branch.

The DR units consist of a resistive element with two current leads welded to its ends, enclosed in a metallic box to discharge magnetic energy in the SC coils. In this design, mild steel is chosen as the material due to its higher resistive temperature coefficient compared to stainless steel, allowing for the exploitation of increased resistance during coil discharge.

The pyrobreaker is a single-action switch that needs refurbishment after use. It should always remain closed under normal and quench conditions. It is actuated only when the CB fails to interrupt the current. Therefore, the design and operation of the pyrobreaker are not covered in this paper.

B. Operation principle

The current commutation process of the proposed FDU scheme for the 45 kA current interruption is shown in Fig. 2 and Fig. 3. The overall process is divided into two phases. Under normal conditions, the BPS and PB carry the normal coil current, as shown in Fig. 2 (a). When a quench occurs and the protection system receives operation signals, the IGCT branch is activated by a turn-on signal, as depicted in Fig. 2 (b). In the meantime, an open command is given to the BPS. However, there is a is a time delay of 200 ms to 300 ms before the BPS contacts start to separate after receiving the command. Hereafter, the arc voltage compels the current to commute from the BPS to the IGCT branch, as shown in Fig. 2 (c). The arc voltage, dependent on the contact distance and typically ranging from 20 V to 60 V [23]. Phase 1 completes when the current is fully transferred to the IGCT branch, and the BPS is fully separated, as shown in Fig. 2(d).

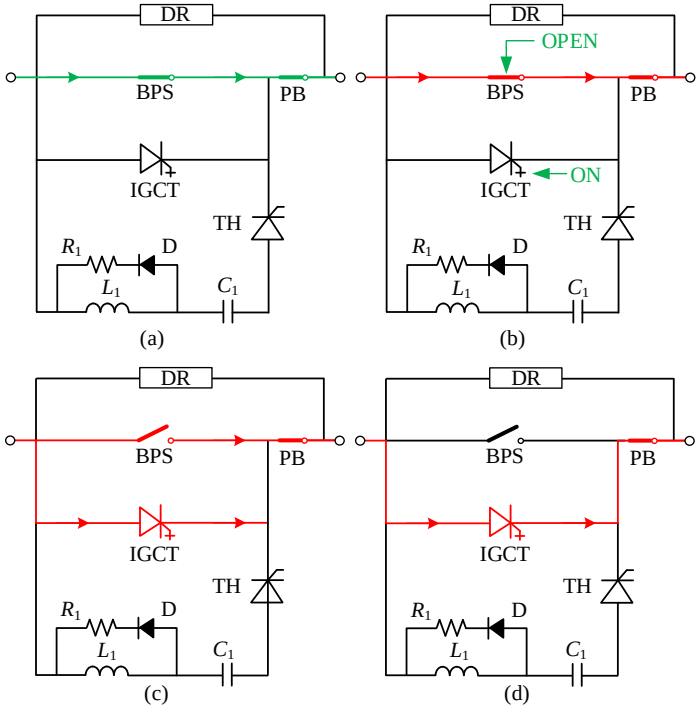

Fig. 2 The first phase of the current commutation process of the proposed FDU. (a) State 1. (b) State 2. (c) State 3. (d) Phase 4.

After completing the first phase mentioned above the FDU has two options for current commutation into the DR. In accordance with the preliminary plasma requirements, the plasma ramp-up duration spans from 100s to 200s, and the plasma ramp-down duration exceeds 150s. Within these intervals, the coil current is mostly falling below the rated value in theoretical. Therefore, the IGCT branch is directly commanded to turn-off to effectuate current commutation into the DR under such conditions. Noting that in practical experiments, the current in CS and PF coils consistently remains below the rated value even during flat-top process. Nonetheless, the rated current holds crucial significance and is considered.

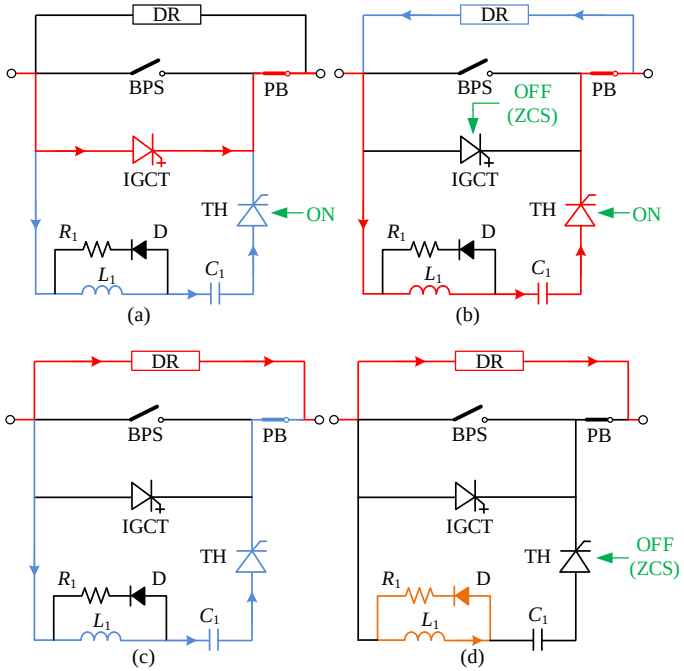

Fig. 3 The second phase of the current commutation process of the proposed FDU. (a) State 1. (b) State 2. (c) State 3. (d) State 4.

If the quench occurs during the flat-top interval, the thyristor branch turns on to provide the current pulse path, L_1-C_1-THs. The designed *LC* circuit generates a reverse pulse current to reduce the current in the IGCT branch, as shown in Fig. 3 (a). It is worth noting that the resistance of the IGCT branch is significantly lower than that of the DR. Therefore, the reverse current is flowing through the IGCT branch during this interval, with the peak current exceeding 45 kA. As shown in Fig. 3 (b), when the current decreases to zero, and IGCTs are turned off under ZCS conditions to prevent the gate voltage oscillations and current sharing issues. Hereafter, the reverse current in thyristors decreases, as shown in Fig. 3 (c). Lastly, the thyristor branch is turned off under ZCS conditions (Fig. 4 (d)). As a result, the current is commuted to the DR completely, and the energy stored in L_1 is discharged through R_1 and diodes.

The above description outlines the operational principle of the proposed FDU scheme. In comparison to the ITER-like design, the proposed scheme eliminates the need for VCBs, resulting in arc-less current interruption. Moreover, the IGCT branch exhibits promising maintainability, controllability, and rapid current interruption capability. In low-current quench scenarios, the IGCT can still interrupt the current rapidly. Compared to the JT-60SA-like scheme, the proposed FDU can achieve zero current switching (ZCS) for IGCTs and thyristors. Therefore, the proposed FDU not only mitigates driving and current sharing issues but also enable enhanced reliability of IGCTs. The parameter design is analysed in the next section.

II. Feasibility study and parameters design

A. The analysis of the first phase and IGCT branch design

*phase*The reliable current communication from the BPS branch to IGCT branch is important for proposed FDU, which is the is the first step for the two current interruption options. Assuming R_{BPS} and L_{BPS} are the equivalent resistance and stray inductance of the BPS branch, respectively. Analogically, R_{IGCT} and L_{IGCT} are the resistance and inductance of IGCT branch. V_{arc} is the arc voltage of the BPS. Therefore, the first phase of the current commutation process can be illustrated in (1).

$$\begin{cases} i_{BPS} + i_{IGCT} = i_{SC} \\ L_{BPS}\dfrac{di_{BPS}}{dt} + i_{BPS}R_{BPS} + V_{arc} = L_{IGCT}\dfrac{di_{IGCT}}{dt} + i_{IGCT}R_{IGCT} \end{cases} \tag{1}$$

According to (1), it is known that to achieve a complete and safe current commutation requires $R_{IGCT} < V_{arc}/I_{SC}$. The detailed analysis of this process is illustrated in [19] and [23], and it is not repeated in this paper.

The design of the IGCT branches should account for both the current interrupting capability and the reapplied voltage. The current design constraints for the CS/PF FDU are outlined in [24]. The nominal and maximum voltage terminal-to-terminal during current dump (normal operation, no fault) should be below 20 kV, while the nominal and maximum terminal voltage-to-ground during current dump (normal operation, no fault) should be below 10 kV. In this design, the IGCT module 5SHY42L6500 (4 kA, 6.5 kV) is considered. According to the proven design criteria in [23], 8 IGCTs in parallel can interrupt 25.7 kA, with nominal reapplied voltage of 3.8 kV and sufficient margin for current sharing and malfunction of 1 IGCT . Therefore, in this design, the IGCT-based CB comprises 14 IGCT branches connected in parallel, with each IGCT branch consisting of 5 IGCTs connected in series.. Notably, the proposed FDU scheme can be upgraded to match the current rating of 74.6 kA, in line with the current rating of TF coils. However, a key challenge for TF FDUs in DEMO is the compatibility with the neutron and gamma radiations foreseen in the tokamak basement. Therefore, the power electronics parts (IGCTs and CPC) in the proposed FDU should be placed in more shielded areas, following industrial best practices. The feasibility and RAMI of this solution is still under evaluation.

B. The analysis of the second phase

*phase*For the second phase of current commutation, it is important to ensure the peak value of the reverse current exceeds 45 kA to achieve the ZCS of IGCT and thyristor branch. The reverse pulse current i_{TH} is determined by the value of capacitor, inductor, and the pre-charged voltage of the capacitor. A ZCS factor k_{ZCS} is defined as 1.2 to ensure the reliable ZCS. Therefore, the peak value of the reverse current

generated by the CPC is 55 kA. The thyristor-triggered CPC is a well-established technology has been used in SC magnets (see TABLE I). Therefore, only the parameter design is discussed in this section, and the topology and connectivity configuration are not detailed in this paper.

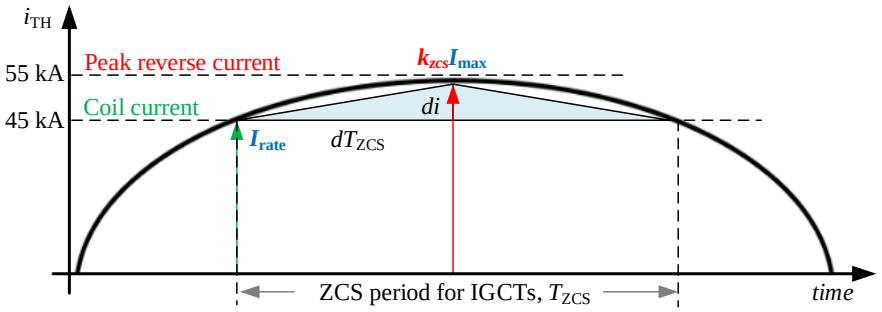

Fig. 4 The waveform of the reverse current generated by the thyristor-triggered CPC.

The waveform of the reverse current is shown in Fig. 4. To achieve the successful ZCS, it is important to ensure a sufficient ZCS period of T_{ZCS}. Therefore, the time derivative of the reverse current should be properly limited. Therefore, the parameters of the CPC can be designed as:

$$\begin{cases} U_{C1} = k_{ZCS} \cdot I_{rate} \cdot \sqrt{\dfrac{L_1}{C_1}} \\ L_1 = \dfrac{U_{C1}}{\left| di / dz_{CS} \right|}, \ \left| \dfrac{di}{dz_{CS}} \right| \le 300 \ (A/us) \end{cases} \tag{2}$$

Based on the above analysis, the parameters of the *LC* circuit are given in TABLE II.

TABLE II. Parameters of the *LC* Circuit

Parameter	Item	Value
Pre-charged voltage of C_1	U_{C1}	5 kV
Capacitance of C_1	C_1	2.02 mF
Inductance of L_1	L_1	16.67 uH
ZCS factor k_{ZCS}	k_{ZCS}	0.85

C. The discharge resistor design

The proposed FDU scheme adopts the ITER-like DR design [25]. The DR is based on a unified resistor section as shown in Fig. 5. It comprises a resistive element with two current leads welded to its ends, which enclosed within a metallic box. The resistive element is made of a mild-steel tape (1 mm width) in a tight zigzag pattern.

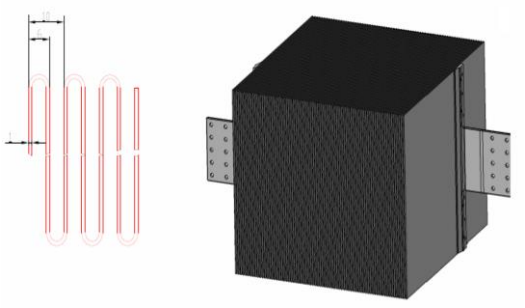

Fig. 5 The unified ITER-like DR section [25].

The DR is made of mild steel, known for its higher resistive temperature coefficient compared to stainless steel. Therefore, for the same amount of I^2t, the voltage peak applied to the coil is reduced. In

this design, the thermal coefficient for the mild steel is assumed to be same as ITER, which is β = 4.6e-3/K^{-1}. The parameters for an individual resistor are outlined in TABLE III [25].

TABLE III. Parameters of the Resistor Module [25]

Parameter	Value	Unit
Rated energy	220	MJ
Peak current	17	kA
Resistance at 20 °C, R_m	0.025	Ω
Mass of conductor (m)	517	kg
Dimensions (L×W×H)	0.75/ 0.75/ 0.58	m
Max temperature, T_{MAX}	300	°C

The resistor module exhibits a peak current of 17 kA, which implies the parallel arrangement of at least three modules to meet the nominal current peak of 45 kA for the CS/PF coils in DEMO.

To fulfill the requirements of DEMO, it is imperative to determine the optimal configuration regarding the number of resistor modules connected in series and in parallel. Taking the CS coil, CS3U, as an example, the self-inductance of the coil is 3.461 H. The required discharge time constant is 7.5s, and a total I^2t of 7.59 GA^{2}s. Considering the parameters listed in TABLE III, a minimum objective function can be established as:

$$\min f(x) = \left(R_D - R_m \cdot \frac{N_s}{N_p} \right) \tag{3}$$

R_D represents the total discharge resistor at 20℃, which is 0.3667 Ω for CS3u. It is worth to mention that this design accounts for the heating effect of the temperature-dependent resistor during discharge, to satisfy the I^2t but limiting the peak voltage. However, this method works only if the coils are considered separately, i.e. without considering the magnetic mutual couplings among the coils and between the coils and the surrounding passive structures. The mutual coupling among the coils, in particular, can increase a lot the magnetic energy of the system, making difficult to satisfy at the same time the voltage and I^{2}t requirements. Studies are in progress on this regard, considering realistic initial current in the coils according to the available scenarios.

According to (3), the number of sections in parallel N_p = 3, and the number of sections in series N_s = 44. This design method is applied to configure the DR for CS, PF and TF coils in DEMO. The DR design for all CS and PF coils is listed in TABLE IV.

TABLE IV. Parameters of the Resistor Module for CS and PF Coils

CS Coil	N_s	N_p	R_D	PF Coil	N_s	N_p	R_D
CS3U	3	44	0.3667 Ω	PF1/PF2	3	13	0.1083 Ω
CS2U	3	44	0.3667 Ω	PF3	3	44	0.3667 Ω
CS1	3	51	0.425 Ω	PF4	3	44	0.3667 Ω
CS2L	3	44	0.3667 Ω	PF5	3	50	0.4167 Ω
CS3L	3	44	0.3667 Ω	PF6	3	32	0.2667 Ω

The above analysis provides a preliminary design for each main component in the proposed FDU, considering the specific requirements of DEMO. The simulation results based on the above parameters are given and analysed in the next section.

III. Simulation verification

Building upon the feasibility study and parameter design outlined above, simulation tests are carried out in PLECS/Plexim. The proposed FDU scheme is evaluated through two case studies: the CS coil (CS3u) and the PF coil (PF5). The CPC design follows the specifications in TABLE II, and the DR design is derived from TABLE III and TABLE IV. The FDU and system parameters are given in TABLE V.

TABLE V. Simulation Parameters

Item	Value	Item	Value
Coil inductance of CS3U	3.461 H	Discharge resistor R_1	0.5 Ω
Coil inductance of PF5	9.113 H	Initial temperature of DR	40 °C
Peak arc voltage of the BPS	25 V	Specific heat capacity of DR	620 J/(kg*K)
Resistance of the BPS	1.5 μΩ	Heat transfer coefficient of DR	20 W/(m^{2}K)

The current commutation process for CS3U is shown in Fig. 6 (a). The commutation of coil current to the IGCT branch starts at t = 10s. A 150 ms time delay is set for the sufficient movement of contacts in BPS, ensuring a safe turn-off of the BPS. During this period, the arc voltage in the BPS reaches its maximum value. At t = 10.15s, the CPC triggers, compelling a rapid reduction of current in the IGCT branch to zero. Hereafter the current in the CPC is fully transferred to DR after the reverse current naturally decreases to zero. A zoomed-in view of this process is shown in Fig. 6 (b). The ZCS period for the IGCT branch begins when the reverse current increases to 45 kA and ends when the reverse current decreases to the value of 45 kA. The peak value of the reverse current is 53 kA. The parameter design ensures the proper setting of T_{ZCS} = 300 μs, which guarantees a reliable turn-off for the IGCT branch. In addition, it can be observed that the DR provides the current path for the overcurrent, reaching up to 8 kA during T_{ZCS}.

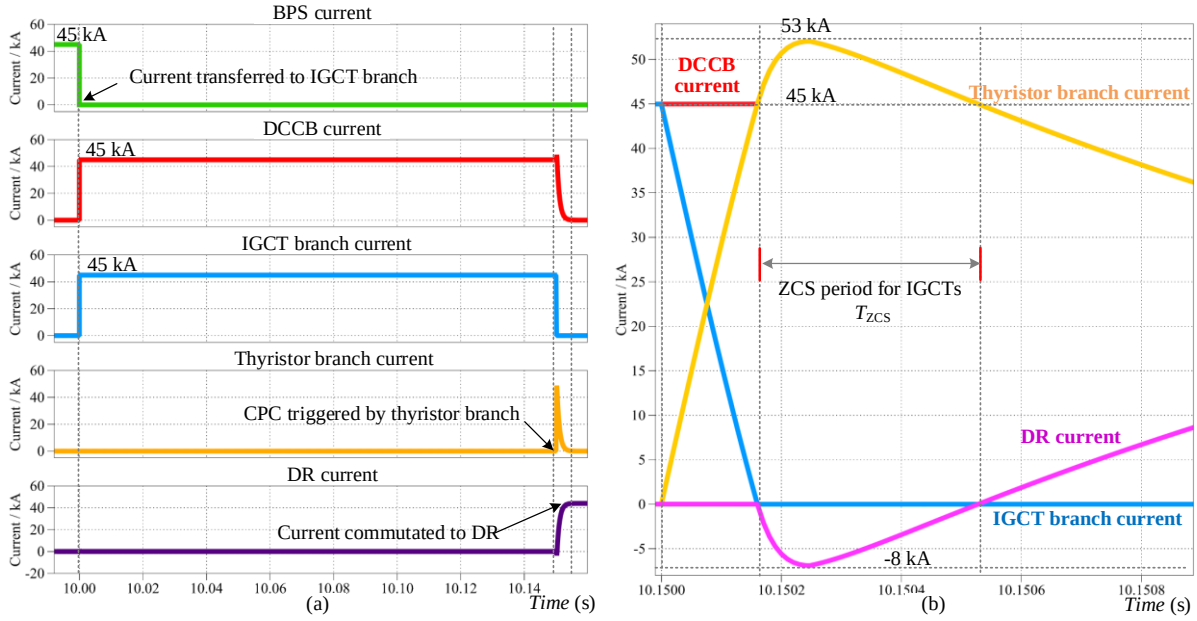

Fig. 6 Current waveforms of the proposed FDU at 20°C. (a) Overview of the current commutation process. (b) Zoomed-in view of the process of current commutated from the IGCT branch to the CPC.

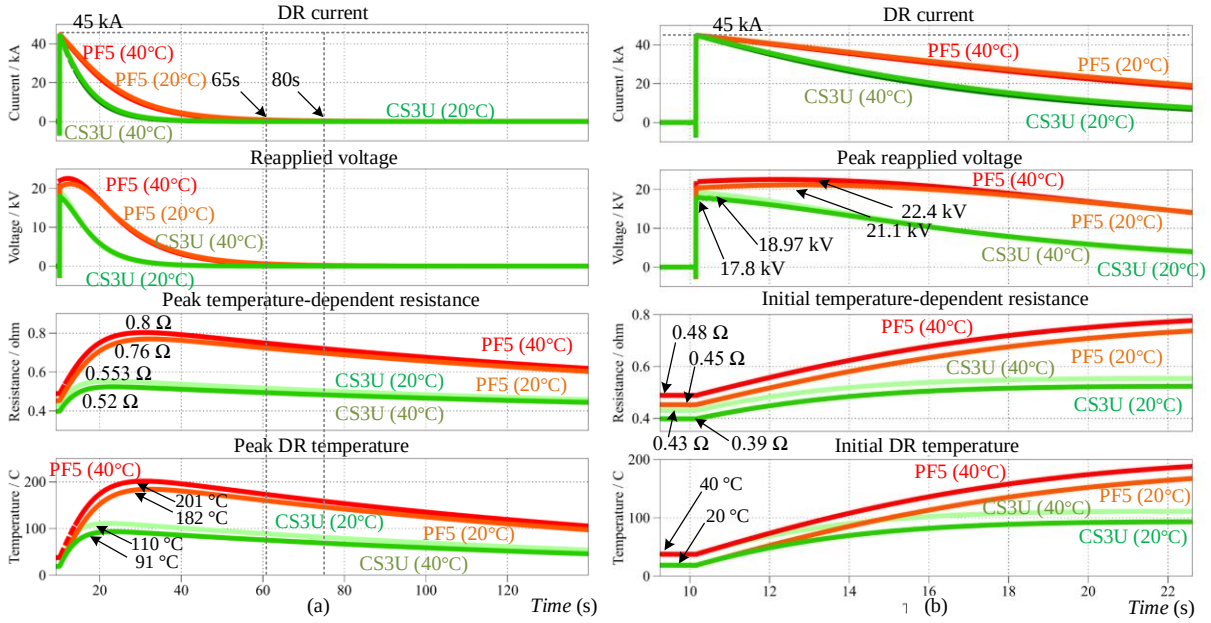

Fig. 7 Waveforms of the DR in CS3U coil and PF5 coil under 20°C and 40°C. (a) Overview of the current discharge process. (b) Zoomed-in view of the process of current commutated from the CPC to the DR.

Fig. 7 shows the waveforms of the DR in the proposed FDU which applied to CS3U and PF5 under different initial ambient temperature conditions (20°C and 40°C). At 20°C, the current in CS3U is completely discharged at t = 60s. Given that the current is commutated to the DR at t = 10.15s (see Fig.6 (b)), the total discharge period is approximately T_{dis_CS3U} = 50s. In comparison, the current in PF5 is completely discharged at t = 85s, and the total discharge period is T_{dis_PF5} = 75s. The peak values of the temperature-dependent resistances for CS3U and PF5 are 0.52 Ω and 0.76 Ω at 20°C, respectively. Furthermore, the rate of change of the two resistors aligns with the temperature variation. The peak temperature of the DR in CS3U is 91°C, and in PF5 is182°C. Both peak temperature values are below the maximum temperature (T_{max}) of 300°C. In Fig. 7(b), the peak reapplied voltage on CS3U is 17.8 kV, and the reapplied voltage on PF5 is 21.1 kV. It is worth mentioning that at the initial instant of current commutation to the DR, the voltage on each coil is lower than its peak value. This confirms the merit of the adopted resistor over constant-resistance resistors. The voltage values are within the designed safe margin of the IGCT branch.

At 40°C, the peak values of the temperature-dependent resistances for CS3U and PF5 are 0.553 Ω and 0.8 Ω, respectively. The peak temperature of the DR in CS3U is 110°C, and in PF5 is 201°C. In Fig. 7(b), the peak reapplied voltage on CS3U is 18.97 kV, and the reapplied voltage on PF5 is 22.4 kV.

By comparing the two cases at different temperatures, it can be observed that the voltage reaches the peak value rapidly in CS3U. This is because the thermal capacitance of the ITER unified resistor section is relatively high compared to the resulting discharge time constant of the coils, resulting in a not significant temperature increase. In addition, it can be seen from Fig. 7 (b) that the initial resistances deviate from the values provided in TABLE IV. This discrepancy is primarily due to the dynamic changes in temperature and resistance induced by the reverse current flow through the DR during T_{ZCS}.

IV. Conclusion

DEMO will go from a science-driven experiment to a public-private partnership project with the involvement of industry from the beginning, which requires advanced technologies and poses high requirements to safely generate power. This implies the adopted technology should not only reach specifications demanded by the industry but also fulfill the RAMI.

Based upon the requirements, a 45 kA/ 20kV soft-switched hybrid DCCB is proposed in this paper. The proposed scheme ensures a reliable ZCS turn-off of the parallel connected IGCTs within a controllable period T_{ZCS}. The tentative design of each main device is provided, including IGCT branch, CPC, and DR. In addition, the current commutation process and parameter design criteria are thoroughly presented. Simulation tests for CS3U coil and PF5 coils are conducted. The preliminary results shows that the proposed FDU scheme can interrupt 45 kA current in CS and PF coils rapidly and safely under high ambient temperature conditions, with a peak voltage of 21.1 kV and 22.4 kV respectively. Furthermore, the temperature-dependent DR effectively reduces the voltage peak applied to the coil. The proposed DCCB is aimed to address key issues and design aspects specific to DEMO, but the design concept is applicable also to other similar applications. The exploration of system reliability, resilience to radiations, economic viability, industrial feasibility, etc., will be further analyzed in the future.

BIBLIOGRAPHY

[1] S. Tosti, "Classical Thermodynamic Analysis of D-Based Nuclear Fusion Reactions: The Role of Entropy," *Energies,* vol. 16, no. 10, May 9, 2023.

[2] J. Sheffield et al., "Physics Requirements for an Attractive Magnetic Fusion-Reactor," *Nucl. Fusion,* vol. 25, no. 12, pp. 1733-1743, Dec, 1985.

[3] K. Okuno, A. Devred, "Technology development for the construction of the ITER superconducting magnet system," *Nucl. Fusion,* vol. 47, no. 5, pp. 456-462, May, 2007.

[4] H. Shirai, P. Barabaschi, Y. Kamada, and J.-S. Team, "Recent progress of the JT-60SA project," *Nucl. Fusion,* vol. 57, no. 10, Oct, 2017.

[5] Y. T. Song et al., "Concept Design of CFETR Tokamak Machine," *IEEE Trans. Plasma Sci.,* vol. 42, no. 3, pp. 503-509, Mar, 2014.

[6] S. Ciattaglia, M. C. Falvo, A. Lampasi, and M. P. Cosimi, "Energy Analysis for the Connection of the Nuclear Reactor DEMO to the European Electrical Grid," *Energies,* vol. 13, no. 9, May, 2020.

[7] M. Huguet, I. J. C. Team, and I. H. Teams, "Key engineering features of the ITER-FEAT magnet system and implications for the R&D programme," *Nucl. Fusion,* vol. 41, no. 10, pp. 1503-1513, 2001.

[8] EUROfusion. "European Research Roadmap to the Realization of Fusion Energy," accessed on 31 December, 2023; https://www.euro-fusion.org/eurofusion/roadmap/

[9] E. Gaio et.al., "Conceptual design of the quench protection circuits for the JT-60SA superconducting magnets," *Fusion Eng. Des.,* vol. 84, no. 2-6, pp. 804-809, Jun, 2009.

[10] E. Gaio et al., "The EU DEMO Plant Electrical System: Issues and perspective," *Fusion Eng. Des.,* vol. 156, Jul, 2020.

[11] E. Gaio et al., "Status and challenges for the concept design development of the EU DEMO Plant Electrical System," *Fusion Eng. Des.,* vol. 177, Apr, 2022.

[12] T. B. Deng, et al, "Multi-coupled commutation analysis in EAST poloidal field quench protection circuits based on fuse model," *Fusion Eng. Des.,* vol. 155, Jun, 2020.

[13] K. Risse, T. Rummel, T. Mönnich, F. Ftillenbach, H. S. Bosch, and W.-X. Team, "Updates on protection system for Wendelstein 7-X superconducting magnets," *Fusion Eng. Des.,* vol. 146, pp. 910-913, Sep, 2019.

[14] E. Gaio et al, "Full scale prototype of the JT-60SA Quench Protection Circuits," *Fusion Eng. Des.,* vol. 88, no. 6-8, pp. 563-567, Oct, 2013.

[15] J. Hong et al, "The operation result of supervisory interlock system for the KSTAR 1st campaign," *Fusion Eng. Des.,* vol. 85, no. 3-4, pp. 500-504, Jul, 2010.

[16] A. Ivanov, et al., "Type tests of counter pulse circuits for the ITER fast discharge units," *Fusion Eng. Des.,* vol. 146, pp. 1934-1937, Sep, 2019.

[17] M. Xu, H. Li, Z. Q. Song, X. G. Hu, C. W. Tang, and P. Fu, "The challenge and solution of overvoltage for 100 kA Quench Protection System in CRAFT project," *Fusion Eng. Des.,* vol. 175, Feb, 2022.

[18] X. G. Hu, H. Li, C. W. Tang, Z. Q. Song, and P. Fu, "A new structure of mechanical switch used for hybrid breaker in quench protection system," *Fusion Eng. Des.,* vol. 171, Oct, 2021.

[19] W. Tong, M. Xu, H. Li, and B. Chen, “The conceptual design of upgraded 100 kA quench protection system for CRAFT superconducting magnet,” *Fusion Eng. Des.*, vol. 187, Feb, 2023.
[20] L. Novello, E. Gaio, and R. Piovan, “Feasibility Study of a Hybrid Mechanical-Static DC Circuit Breaker for Superconducting Magnet Protection,” *IEEE Trans. Appl. Supercond.*, vol. 19, no. 2, pp. 76-83, Apr, 2009.
[21] S. S. Wang et al, “A 15-kA Solid-State Circuit Breaker Research and Development for the Switch Network Unit of the EAST Tokamak,” *IEEE Trans. Plasma Sci.*, vol. 49, no. 9, pp. 2979-2986, Sep, 2021.
[22] S. S. Wang, Z. Q. Song, P. Fu, and H. Li, “Conceptual Design of Bidirectional Hybrid DC Circuit Breaker for Quench Protection of the CFETR,” *IEEE Trans. Appl. Supercond.*, vol. 28, no. 8, Dec, 2018.
[23] E. Gaio, A. Maistrello, L. Novello, M. Matsukawa, M. Perna, A. Ferro, K. Yamauchi, and R. Piovan, “The new technological solution for the JT-60SA quench protection circuits,” *Nucl. Fusion*, vol. 58, no. 7, Jul, 2018.
[24] K. Sedlak, Common operating values for DEMO TF WP design for 2016, v. 1.4, June 21th, 2016.
[25] A. Ferro, et al., Results from first studies on an ITER-like design of the Coil Power Supply System BOP-6-T015-D001, IDM ref. n. EFDA_D_2N7ME8, 2020.